

Refractories Applications *Transactions*

Volume 4, Number 1

March/April 2009

Editorial Board

Jeffrey D. Smith, Editor, Missouri S&T, USA
Mary Lee, Assistant to the Editor, Missouri S&T, USA

Technical Referees

Esteban Aglietti, CETMC, Argentina
Richard C. Bradt, The University of Alabama, USA
Carmen Baudín, Instituto de Cerámica y Vidrio, Spain
Elena Brandaleze, Instituto Argentino de Siderurgia
Angel Caballero, Instituto de Cerámica y Vidrio, Madrid, Spain
William G. Fahrenholtz, University of Missouri-Rolla, USA
Geraldo E. Gonçalves, Magnesita S.A., Brazil
Orville Hunter, Consultant, USA
William E. Lee, University of Sheffield, UK
Li Nan, Wuhan University of Sci. & Tech., China
George Oprea, The University of British Columbia, Canada
Victor C. Pandolfelli, Universidade Federal de São Carlos, Brazil
Christopher Parr, Lafarge Aluminates, France
Jacques Poirier, Polytech, Orleans, France
Michel Rigaud, École Polytechnique, Canada
Charles Semler, Semler Materials Services, USA
Mark Stett, Consultant, USA
Raul Topolevsky, Siderar, Argentina

All submissions should be sent to:

Mary Lee, Assistant to the Editor
Refractories Applications Transactions
Missouri S&T
Materials Science and Engineering Dept.
223 McNutt Hall
1870 Miner Circle Drive
Rolla, MO 65409-0330

Phone: (573) 341-6561
Fax: (573) 341-6934
E-mail: leem@mst.edu

For author guidelines please see those listed on the *Journal of the American Ceramic Society* website: <http://www.ceramics.org/publications/journal/authorinstructions.asp>

File Formats

Text: Microsoft Word.

Graphics: JPEG, TIFF or EPS created from supported applications, PowerPoint, Acrobat PDF (PDF format is acceptable for review purposes only)

Microsoft Word with embedded graphics.

Compression Software: WinZip (PC) or Stuffit (Macintosh)

Resolution of graphics files must be at least 300 dpi for halftones, 600 dpi for lettering, and 1200 dpi for line art.

Manuscript Number 013007

Non-Classical Creep Behavior of Fusion-Cast α/β Alumina Refractories

James G. Hemrick and Andrew A. Wereszczak
MS&T Division, Oak Ridge National Laboratory, Oak Ridge, TN 37831
hemrickjg@ornl.gov

ABSTRACT

The compressive creep of a typical 50% α -/50% β -alumina fusion-cast refractory block was examined. Test temperatures (1450-1650°C) were chosen to correspond to those typical of service conditions. Relatively high compressive test stresses (0.6 and 1.0 MPa compared to 0.2-0.4 MPa which is typical of service) were chosen to promote extensive deformation and to provide for more accurate creep strain measurements. It was found that the measured creep strain responses in this alumina were a sum of (contracting) compressive creep strain and expansive strain attributed to time and temperature dependent microcracking. Long term, isothermal expansion tests conducted in parallel allowed for the deconvolution of the compressive creep and expansive strains present in the measured creep strain. The analysis shows that in spite of complications associated with conflicting expansion and contraction effects, classical creep analysis may be applied to this alumina refractory provided the strains associated with the non-steady-state mechanism are considered.

INTRODUCTION

Tighter environmental standards and cost constraints have driven many industrial glass plants to consider converting older, conventional air-fuel fired furnaces to oxy-fuel firing, or are building new oxy-fuel fired furnaces. Consequently oxy-fuel technology has become the primary technology of interest to the glass industry as it promises not only pollution abatement, but also increased glass pull effectiveness and capital cost savings¹.

Yet, the new internal furnace environment produced by oxy-fuel firing creates many problems with refractory life that were not previously encountered with conventional firing involving air and natural gas. Furnaces employing oxy-fuel firing have increased potential for corrosion and "rat holing" along with deterioration of traditionally used conventional silica crown refractories^{2,3}. Also, more intense alkali attack occurs under this environment as water vapor reacts with alkali from the glass melt and batch to form hydroxide vapors resulting in a significant increase in the concentration of volatiles in the furnace².

Therefore, alternatives to silica-based refractories have been considered for superstructure applications. Fusion-cast alumina (FCA) is one such alternate, but little data exists regarding the characterization of this refractory material. Therefore, there is a need to generate the data essential to both engineering design and performance predictions. The present study attempts to relate the compressive creep behavior of FCA refractory blocks to their respective microstructure as a function of stress and temperature. However, the non-classical creep behavior observed for these 50% α -/50% β -alumina fusion-cast refractories warranted that a non-traditional creep analysis technique be employed to interpret the observations. This paper reports the compressive creep results obtained from the testing

of characteristic bulk samples of FCA and addresses the underlying phenomena believed to be causing the unusual behavior.

BACKGROUND

FCA refractories are formed by melting the batch materials in an electric-arc furnace and then casting in steel or graphite molds. After a shell has solidified forming the exterior of the casting, the blocks (with a still molten core) are removed from their molds and placed in bins surrounded by alumina annealing powder where they are allowed to cool. Complete cooling can take several weeks to months depending on the casting size. The nature of the solidification process promotes the variable microstructure that is characteristic of fusion-cast refractory. Similar to metallic castings, a zone of columnar grains oriented in the direction of cooling (heat flow) on the exterior of the block surrounds a more homogeneous and equiaxed interior⁴. This varying microstructure leads to local differences in physical properties such as thermal conductivity, elastic modulus and creep resistance within a casting. These effects are discussed in greater detail elsewhere⁵.

These refractories are well suited for glass contact exposure since the β -alumina ($\text{Na}_2\text{O}\cdot 11\text{Al}_2\text{O}_3$) crystals are dispersed in size and continuity by α -alumina crystals creating a dense structure with a large average crystal size of several hundred microns⁶. Additionally, these blocks typically possess a low level of porosity (<2%) and a high density ($\approx 3.5\text{g}/\text{cm}^3$)⁶. The literature also reports low intergranular glass contents of less than 1.8 wt% and low levels of impurities (<1 wt% of Fe_2O_3 and TiO_2) coming primarily from processing conditions⁶. Collectively, these properties make fusion-cast alumina highly attractive as a structural material in glass furnace crowns and superstructures as the large grain size and low porosity promote excellent creep resistance.

Since these materials are expected to perform satisfactorily at extremely high temperatures (in excess of 1600°C for many cases), testing must be performed at equivalent temperatures to be meaningful. Additionally, the measured strains during testing are very small because the representative service stresses are low. Therefore, extremely sensitive methods must be employed to experimentally measure those small strains. Furthermore, chemical compatibility between the specimen and test fixture material can become an issue at high test temperatures. Previous testing has shown that standard SiC push-rods react with FCA test specimens when subjected to elevated temperatures. Such reactions alter the test specimen and compromise the validity and accuracy of the resulting creep data.

Analysis of the creep deformation in this material initiated with assuming applicability of classical creep theory as defined by the Norton-Bailey-Arrhenius (NBA) equation is shown below.

$$\dot{\epsilon} = A\sigma^n \exp\left(-\frac{Q}{RT}\right) \quad (1)$$

where: $\dot{\epsilon}$ = strain rate (h⁻¹)

A = constant

σ = stress (Pa)

n = stress exponent

Q = activation energy (J/mol)

R = gas constant (8.314 J/(mol * K))

T = temperature (K)

When creep deformation is well-represented by this theory, an extensive, secondary creep regime will exist from which a steady-state creep rate can be determined. This form of creep will be termed “classical”, while deformation which deviates from this creep representation is termed “non-classical” in this study. Examples of refractory materials that creep “classically” at stresses typical of service include CaO/SiO₂-containing MgO refractories, mullite refractories, and fused silica refractories⁷. Other refractory materials, such as conventional sintered silica, have been shown to follow “non-classical” creep deformation trends⁷.

Both “classical and “non-classical” behavior can be represented by **Equation 2**. It simply states that the measured strain is a sum of all strain activity occurring during testing. In the case of the results discussed in this paper, it was observed that the measured strain was a combination of actual negative creep strain associated with the material being in equilibrium and the contraction in response to the applied compressive stress (ϵ_{creep}) along with a positive strain component (represented as $\epsilon_{\text{expansion}}$) associated with the material being in a non-equilibrium state (i.e., a non-equilibrium state which produced stress-independent bulk expansion).

$$\epsilon_{\text{measured}} = \sum \epsilon_i = \epsilon_{\text{creep}} + \epsilon_{\text{expansion}} \quad (2)$$

For “classical” creep behavior the material can be considered to be in a state of nearly complete equilibrium, therefore $|\epsilon_{\text{creep}}| \gg |\epsilon_{\text{expansion}}|$. Because $|\epsilon_{\text{creep}}|$ is much larger than $|\epsilon_{\text{expansion}}|$, the conventional power-law creep analysis (i.e. application of the NBA equation) is possible. Measured “non-classical” creep, on the other hand, presents a situation where the material is not near a state of equilibrium, therefore $|\epsilon_{\text{creep}}| \leq |\epsilon_{\text{expansion}}|$. For this case, the NBA equation is not sufficient for representing the complex behavior caused by the presence of the non-equilibrium state without additional manipulation of the data.

If one subtracts the effects of the expansion ($\epsilon_{\text{expansion}}$) from the measured creep data ($\epsilon_{\text{measured}}$) in the “non-classical” case, a deconvoluted curve can be produced which then can be analyzed using the NBA equation. This curve should exhibit a non-zero secondary strain rate similar to the “classical” condition and should represent the actual creep (ϵ_{creep}) experienced by the test sample. It is this curve that represents the actual “creep” condition of the material.

The expansion effects present in the measured “non-classical” creep behavior can be caused by any combination of several mechanisms (phase changes, porosity changes, etc.). In previous studies⁸, phase transformations were reported to cause an “unrecoverable expansion” effect in conventional silica refractories. This resulted in the counter-intuitive result of compressive creep samples which were actually larger after testing than they were prior. In silica, it was shown that tridymite reverts to cristobalite during thermal exposure resulting in a positive volume change and thus accounts for the expansion and explains why a measured “non-classical” creep response is observed in this material.

A similar “unrecoverable expansion” has been observed in FCA³. During prolonged exposure (hundreds of hours) to temperatures in the range of 1450-1650°C, “unrecoverable expansions” of 0.2-0.4% were

measured. Although there is silica present in the grain boundary phase of the fusion-cast alumina refractory, it only constitutes a small portion of the overall composition (≈ 1 wt%). Expansion attributable to the phase changes in this small amount of silica would result in a maximum expansion of $\approx 0.002\%$, much less than the expansions measured for FCA products subjected to extended thermal exposure. Additionally, there is a phase transformation possible for FCA refractories. Sodium rich β -alumina ($\rho = 3.25$ g/cm³) can revert to a sodium deficient α -alumina ($\rho = 3.46$ g/cm³) during thermal exposure resulting in a negative volume change. Therefore additional mechanism(s) must be operating to account for the observations.

Thermal expansion hysteresis observed in cyclic dilatometry resulting from microstresses or microcracking may be an indication of such a mechanism. As described by Kingery et al.⁹, residual stresses may develop in a material from differences in thermal expansion coefficients between constituents or from crystallographic anisotropy. These stresses may remain residual or may be sufficient to cause microcracking. Both conditions may lead to thermal expansion hysteresis as these stresses are relieved or the cracks close during cyclic heating. Such hysteresis has been seen in hexagonal materials such as titania⁹ and graphite¹⁰ and has been shown to be predominant in large-grained samples. For such large-grained anisotropic ceramics, a “critical grain size” has been derived and experimentally observed at which materials with grains smaller than the critical size will not form microcracks and materials with grains larger than the critical size are prone to form microcracks^{11,12}. This “critical grain size” is defined to be on the order of 70 μm for Al₂O₃¹³. It is further shown by Adams et al.¹⁴ that pre-existing microcracking exists in many bonded alumina-containing refractories, although fusion-cast materials have not been analyzed for such features.

EXPERIMENTAL PROCEDURES

A fusion-cast alumina block (50% α -/50% β -alumina) with an average grain size on the order of 200 μm and approximate dimensions (0.60 x 0.50 x 0.30 m) was commercially prepared under normal commercial processing conditions. The block was sectioned to obtain creep samples (cylindrical dimensions: 38 mm diameter, 76 mm length) from a location representative of the equiaxed center region of the block.

Compressive creep testing was performed using a frame consisting of a resistance-heated clamshell furnace capable of 1750°C and a pneumatically controlled load cell capable of up to 4500 N. M-type fusion-cast alumina was used to fabricate push rods for the load train, and both a linear variable differential transformer (LVDT) and a contact extensometer were employed as censoring for monitoring axial dimensional changes in the test specimen. Creep tests were accomplished using digitally controlled pneumatic power (by LabVIEW™ software, National Instruments, Austin, TX). Temperature fluctuations were approximately $\pm 2^\circ\text{C}$ to comply with ASTM guidelines¹⁵ and load fluctuations were less than 1% of test load. The specimen was compressed by two push-rods with the unheated ends connecting to water-cooled anvils. The upper compression anvil was fixed to the upper platen by a universal joint and leveled using four turnbuckles. The lower compression anvil rested on an active self-aligning coupler that plays a critical role in maintaining load-train stability and uniform compression. Additional details of the compressive creep system are given elsewhere¹⁶.

Tests were performed in ambient air at 1450, 1550, and 1650°C with applied stresses of 0.6 and 1.0 MPa for durations of 200–300 hours. These temperatures were characteristic of normal operation for oxy-fuel glass tanks currently in service (as specified by the glass manufacturing community). However, the stresses at which testing was performed are intentionally high relative to expected service exposure. A standard crown refractory is only expected to experience stresses on the order of 0.2 MPa, but may be under static loading in a furnace campaign lasting many

* The material discussed in this work showed bulk expansion, but hypothetically **Equation 2** would still apply for a material exhibiting a non-equilibrium bulk contraction.

months or even years. At such low stresses, very small amounts of accumulated strain are produced (on the order of 1% or less).

Stresses of the magnitudes employed in this study are expected to result in greater amounts of creep deformation that is experimentally easier to measure. It is expected that these values may be extrapolated down to the expected in-service stress regime (≈ 0.2 MPa) with little or no error from the data obtained at these higher stress levels assuming that the stress exponent is constant. Yet, small measured amounts of strain are still expected. Therefore, a method of strain measurement is needed that is both extremely precise and which possesses excellent long-term stability. Extensometry has been shown to be such a method^{7, 17}. In addition, a LVDT is utilized as a complementary method of measurement to ensure alignment, monitor creep, and any settlement of the load train.

The cylindrical specimens described above were encased in a fine-grained (100% β -alumina) fusion-cast alumina shell (illustrated in Fig. 1) to inhibit soda evolution from the test specimens into the furnace atmosphere during testing. This is a problem since β -alumina is thermodynamically driven to revert to α -alumina during exposure at elevated temperatures ($>1000^\circ\text{C}$) as the Na atoms in the β -alumina structure become highly mobile and leave the structure¹⁸. As a result, when in service at high temperatures the covering of the refractory by glass will isolate it from the volatilizing alkali environment of the furnace and will cause β -alumina crystals to revert to α -alumina thereby releasing Na into the atmosphere of the furnace¹⁹. This also occurs during testing when these refractories are heated in ambient air since there are no alkali present in this environment to inhibit Na evolution. Consequently, a pure α -alumina layer eventually develops on the exposed surfaces of the refractory with sufficient thickness to inhibit further evolution of sodium from the interior regions of β -alumina. Despite this passivation, the original creep sample becomes modified chemically and microstructurally into a material other than the subject of investigation. Therefore, a β -alumina encasement practice was developed.

The success of a β -alumina shell at inhibiting soda evolution is based on the theory that β -alumina has a relatively high soda content (compared to that of the α/β -alumina specimen) and will provide a relatively high partial pressure of soda adjacent to the exterior of the specimen. Compared to

testing in ambient air, soda evaporation in this arrangement is thermodynamically unfavorable. This theory has been substantiated by microstructural characterization of FCA materials heated in air with and without such a shell arrangement.

Long-term thermal stability (in the absence of an applied stress) was evaluated using a frame consisting of a furnace capable of 1750°C enclosing a dual-rod dilatometer to monitor linear changes in the dimensions of a cylindrical test specimen (38 mm length, 13 mm diameter) taken from the equiaxed bulk region of the commercially prepared block. The specimen was supported by a high purity alumina disk resting on a fixed SiC push-rod while the test assembly was supported by the body of the furnace. The test assembly for monitoring the linear dimensional changes consisted of two sapphire rods in contact with individual linear variable differential transformers (LVDT) and parallel to one another within a sheath of insulation (as shown in Fig. 2).

The linear sample dimension (length) of the tested specimens was continuously monitored using the LVDT in contact with the sample. The initial and final values of the LVDT at room temperature were compared, as well as before and after dimensions of the sample, to ascertain any unrecoverable expansion of the sample associated with the thermal treatment. This change was compared to any unrecoverable expansion sampled by the second (control) LVDT.

Lastly, deconvoluted creep curves were produced by subtracting the measured expansion curves (as measured by the dilatometry technique) from the measured creep curves. Creep analysis using the NBA equation was then applied to these deconvoluted curves.

RESULTS AND DISCUSSION

As expected, all samples showed an increase in diameter associated with the compressive creep testing. Counter-intuitively, all of the tested creep samples exhibited a greater length after compressive creep testing with the exception of the samples tested at $1650^\circ\text{C}/1.0$ MPa, which showed contraction. This measured "non-classical" creep response, related to the increase in length, provided the motivation for interpreting this response using Equation 2. The sample expansion was supported by the dilatometry measurements which showed unrecoverable expansion of test specimens by 0.10% at 1450°C (100 hour soak at temperature), 0.18% at 1550°C (100 hour soak at temperature), and 0.40% at 1650°C (100 soak time at temperature). Testing consisting of heating the sample to 1450,

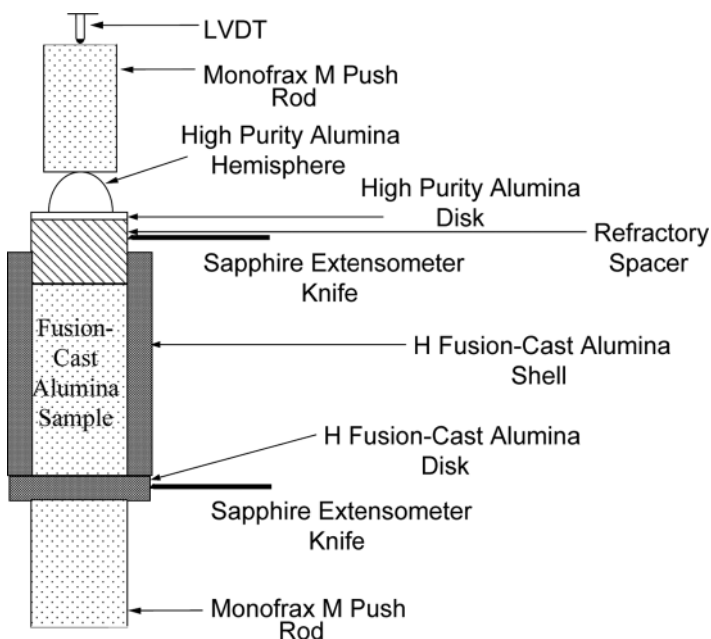


Fig. 1. Creep specimen assembly with H-shell arrangement.

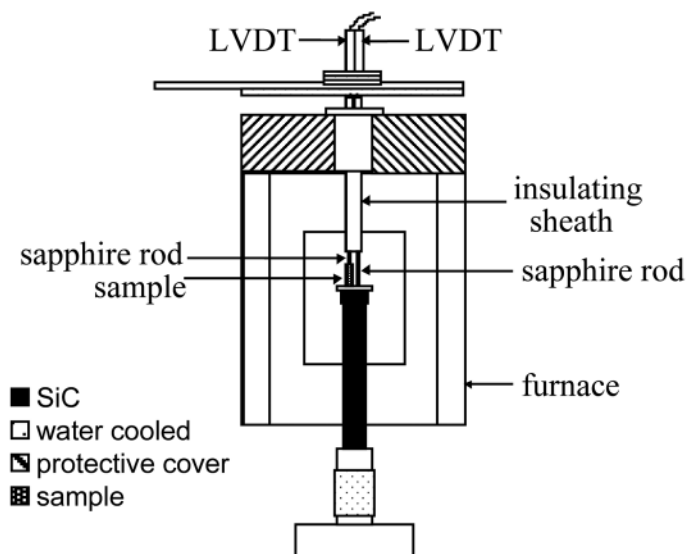


Fig. 2. Test assembly for thermal stability testing.

1550, or 1650°C and immediately returning to room temperature through natural cooling resulted in no measured unrecoverable sample expansion; indicating that the expansion occurred during thermal exposure and not during heating or cooling.

Testing at 1450°C produced the curves shown in **Fig. 3**. Thermal stability testing resulted in 0.114% expansion over a 200 hour time period. Over the same period, creep samples contracted by 0.046% and 0.094% under stresses of 0.6 and 1.0 MPa, respectively. Shapes of the creep curves take on the form of a rapid period of strain accumulation followed by a leveling off of the accumulated strain to a point of near zero strain rate. This is considered “non-classical” creep behavior as described above. Therefore, the NBA equation can not be used directly to accurately evaluate these curves. Upon subtraction of the expansion data from the measured strain curves, deconvoluted curves are produced that exhibit standard non-zero secondary creep rates. Rates were calculated by linearly fitting the secondary regime portions of the curves and analyzing the slopes of the resulting lines. This analysis yielded the minimum creep rates shown in **Table 1**.

Testing at 1550°C produced the curves shown in **Fig. 4**. At this temperature, thermal stability testing produced 0.198% expansion over a 200 hour time period. In the same time period, creep samples contracted 0.038% and 0.090% at 0.6 and 1.0 MPa, respectively. Shapes and magnitudes of the creep curves were similar to those seen at 1450°C resulting in measured “non-classical” creep behavior again being present. As before, the NBA equation could not be used directly to accurately evaluate these curves, but upon subtraction of the expansion data from the measured strain curves, deconvoluted curves were produced that exhibited non-zero secondary creep rates. Analysis was carried out as described above yielding the minimum creep rates shown in **Table 1**.

Table 1. Minimum steady-state creep rates from deconvoluted curves

Temperature (°C)	Stress (MPa)	Creep Rate (h^{-1})
1450	0.6	1.51×10^{-6}
	0.8	1.63×10^{-6}
	1.0	1.75×10^{-6}
1550	0.6	2.05×10^{-6}
	0.8	2.17×10^{-6}
	1.0	2.84×10^{-6}
1650	0.6	2.74×10^{-6}
	0.8	2.90×10^{-6}
	1.0	4.56×10^{-6}

(note: 0.8 MPa data included for completeness)

Testing at 1650°C produced the curves shown in **Fig. 5**. Thermal stability testing produced 0.430% expansion over a 200 hour time period. Over this same period, creep samples contracted 0.093% and 0.242% at 0.6 and 1.0 MPa, respectively. The shape of the curve at 0.6 MPa was similar to that seen previously at 1450°C and 1550°C and was characterized as measured “non-classical” creep behavior for which the NBA equation was not directly applicable. Similar to the earlier analysis, upon subtraction of the expansion data from the measured strain curve, a deconvoluted curve was produced which exhibited a non-zero secondary creep rate as shown in **Table 1**. The 1.0 MPa curve shows an increase in accumulated strain followed by a region of accumulated strain characterized by a constant negative slope. Thus, this test exhibits what is accepted as apparent “classical” creep behavior. The expansion curve was still subtracted from the measured strain curve to produce a deconvoluted curve representative of the actual creep strain (ϵ_{creep}) experienced by the sample. After producing the

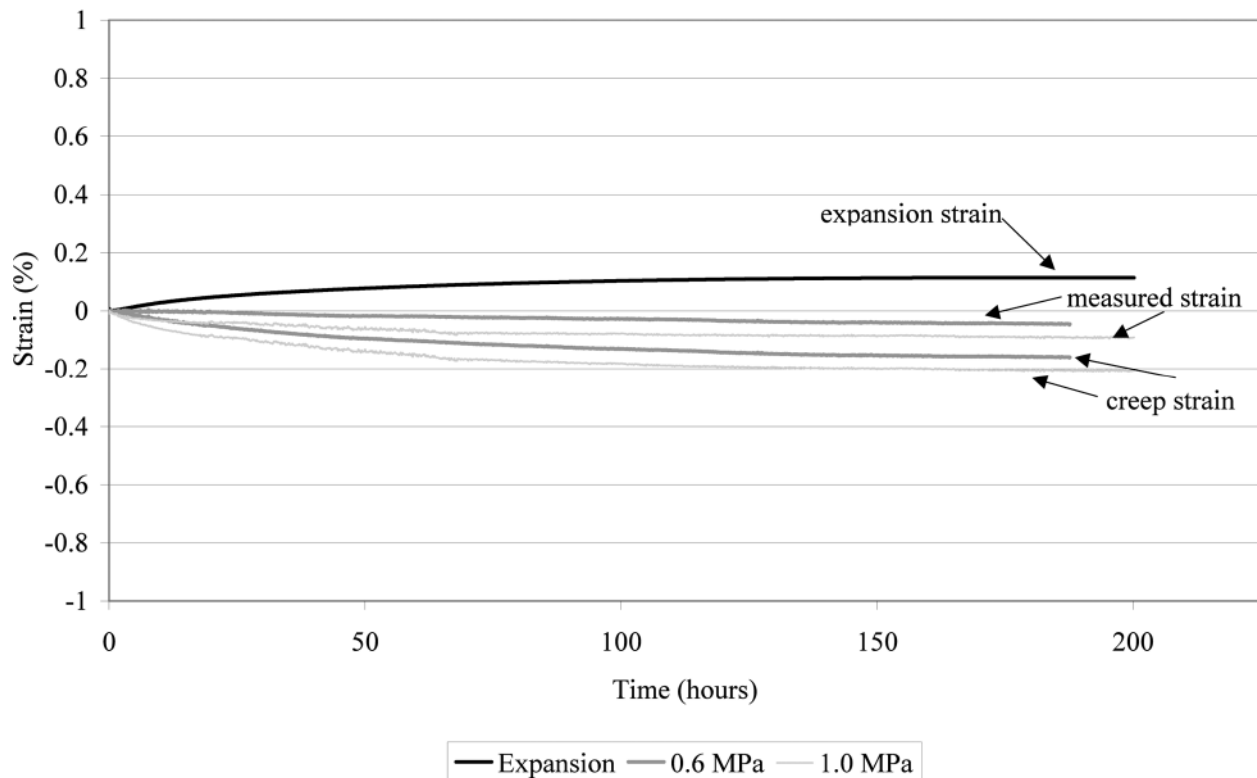


Fig. 3. Measured expansion and creep strain along with deconvoluted curves at 1450°C.

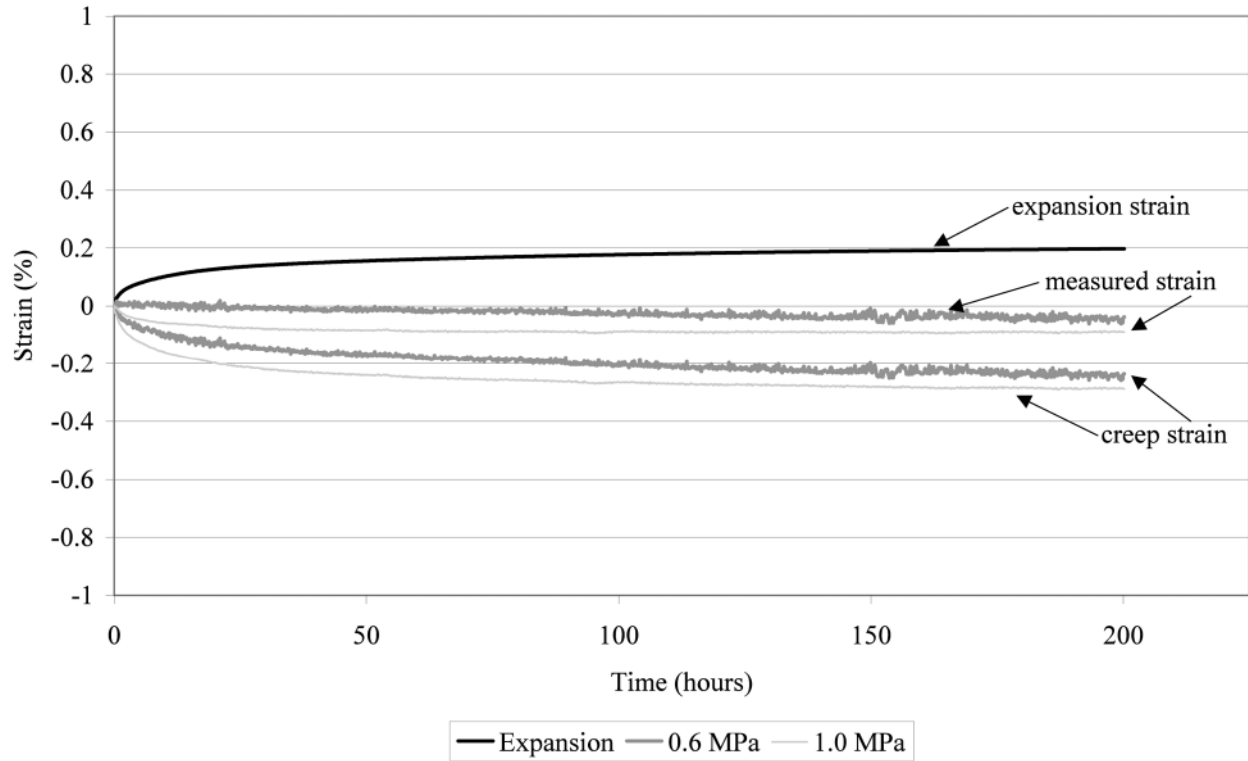


Fig. 4. Measured expansion and creep strain along with deconvoluted curves at 1550°C.

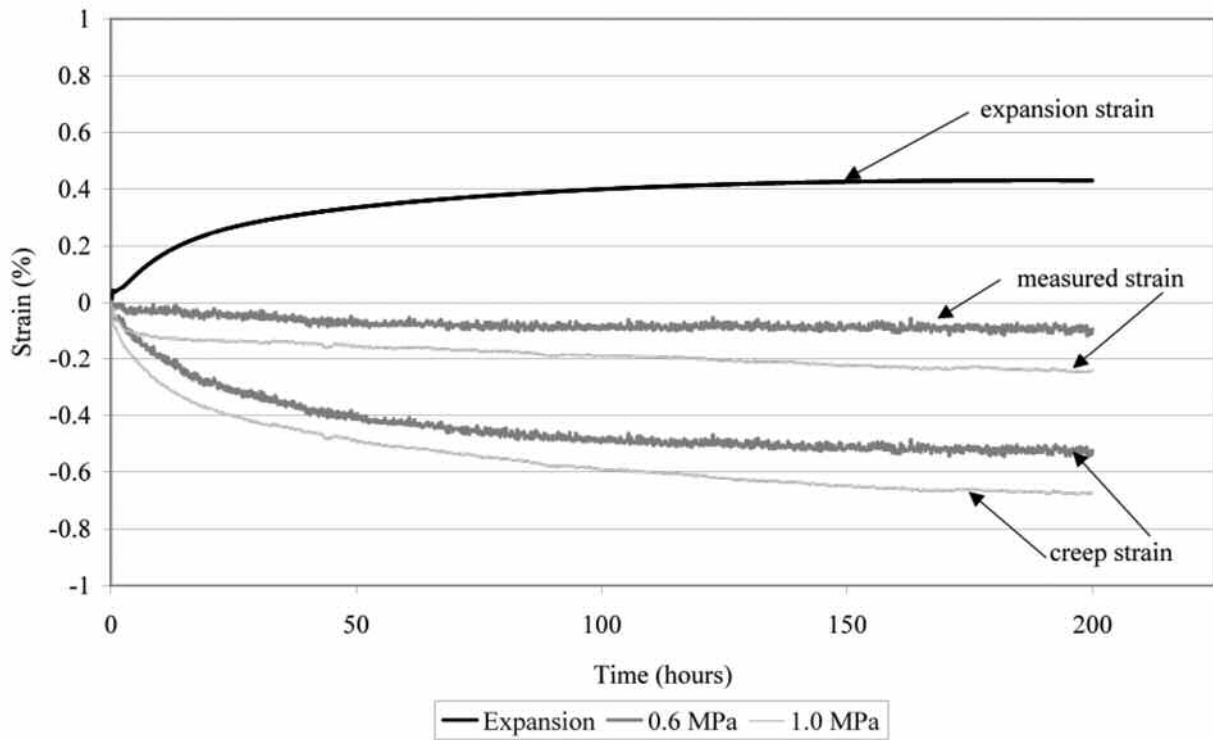


Fig. 5. Measured expansion and creep strain along with deconvoluted curves at 1650°C.

deconvoluted curve, the NBA equation was applied to the analysis. The resulting calculated strain rate is shown in **Table 1**.

Stress exponents and activation energies were calculated from the minimum creep rate data (shown in **Fig. 6**) by performing multiple linear regression on information from multiple stresses and temperatures. This analysis produced a calculated activation energy of -25.56 kcal/(mole*RT) and a stress exponent of 0.64. Both of these values are lower than expected. The reported activation energy for fine-grained alumina is on the order of -130 kcal/(mole*RT), while for diffusional creep of ceramics, a stress exponent of ≈ 1.0 is expected²⁰. This would seem to indicate that multiple mechanisms are controlling the creep behavior of this material at the different temperatures and stresses. This further complicates the use of the NBA equation for characterizing the behavior of this material system.

The effect of unrecoverable expansion of the specimens during exposure to temperature is important. This effect has not only been seen in previous thermal expansion testing⁵, but also in the creep samples described in this work. As mentioned previously, all samples with the exception of the 1650°C/1.0 MPa samples increased in length as well as diameter as a result of thermal exposure during creep testing. The linear increase generally ranged from 0.1-0.2%. Only at the most extreme condition was the creep strain great enough for samples to actually show the intuitive expectation of a linear reduction in size after creep testing.

The presence of this phenomenon is thought to be the cause of the apparent “non-classical” creep behavior seen in all compressive creep testing performed on this material at temperatures and loads up to 1650°C and 0.8 MPa. It has been shown that as temperature increases, the amount of unrecoverable expansion also increases and that when samples are heated and immediately cooled with no hold time at temperature, no unrecoverable expansion occurs⁵. This would indicate that the mechanism causing this effect occurs during the prolonged exposure of the sample to high temperatures and is therefore influential during both creep testing and in service during a furnace campaign. Although not investigated in this work, FCA materials are likely inherently microcracked as a result of the combination of a rapid initial cooling cycle prior to being placed in the alumina annealing bin and the relatively large grain size (on the order of several hundred microns) this material possesses. As discussed previously, such microcracks are known to be prevalent in non-cubic materials (including alumina) and are shown to lead to thermal expansion hystere-

sis of the scale which would account for the unrecoverable expansion reported here.

Furthermore, elastic modulus testing of these materials displays trends also characteristic of materials containing microcracks⁵. It has been shown that brittle materials containing microcracks will experience a depression in elastic modulus attributable to the presence of the cracks²¹⁻²⁴ similar to a heterogeneous composite structure consisting of a solid matrix containing elliptical voids^{25,26}. This effect has also been specifically shown for the case of microcracked alumina at high temperatures²⁷. These microcracks then heal during thermal exposure and a higher elastic modulus is measured at elevated temperatures as well as during cooling of the heated samples. This trend illustrated in **Fig. 7** shows the room temperature elastic modulus measurements for FCA samples before and after a thermal exposure.

CONCLUSIONS

An unrecoverable expansion phenomenon is occurring in the fusion-cast alumina compressive creep samples described in this paper. Thermal expansion hysteresis caused by the presence of microcracks in the fusion-cast alumina samples is thought to be leading to this unrecoverable expansion phenomenon. This effect is believed to be responsible for the apparent “non-traditional” creep behavior which can not be characterized by traditional methods such as the direct use of the Norton-Bailey-Arrhenius (NBA) equation. Through the use of a revised equation incorporating the sum of the strain attributable to compressive creep and the strain associated with unrecoverable expansion resulting from time and temperature dependent microcracking, it was possible to deconvolute the compressive creep response from the expansion effects present in the as-measured strain test data. This allows for the subsequent use of the NBA equation to represent the actual creep response exhibited by this material.

Therefore, in spite of complications associated with conflicting expansion and contraction effects, classical creep analysis may be used with this alumina refractory (and possibly other materials exhibiting such complex creep behavior) after the strains associated with the non-steady-state mechanisms are considered. However, the activation energy and stress exponents derived from the minimum creep rates were lower than expected. This may indicate that multiple rate-limiting mechanisms control the strains of fusion-cast alumina materials under these experimental conditions.

ACKNOWLEDGMENTS

The authors would like to acknowledge the U. S. Department of Energy, Assistant Secretary for Energy Efficiency and Renewable Energy, Office of Industrial Technologies, Advanced Industrial Materials Program and the Glass Vision Team, under Contract DE-AC05-00OR22725 with UT –

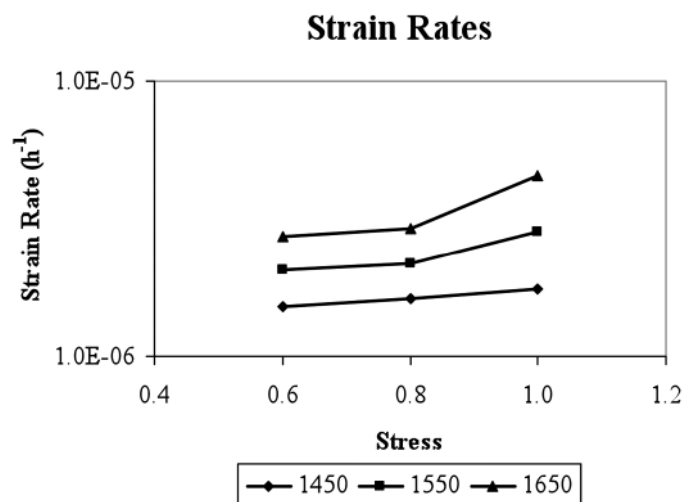


Fig. 6. Minimum strain rates calculated from deconvoluted strain curves. (note: 0.8 MPa data included for completeness)

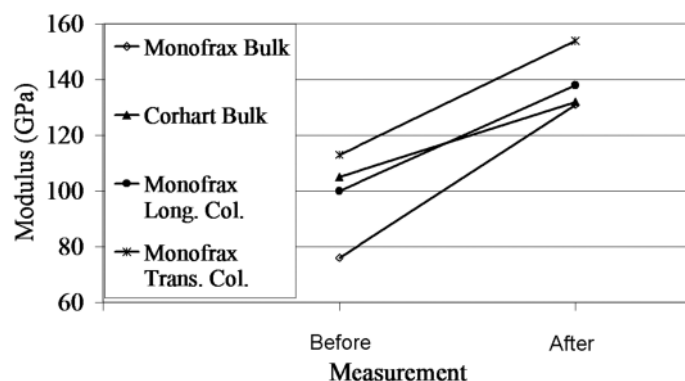


Fig. 7. Room temperature elastic modulus measurements for fusion-cast alumina samples before and after thermal exposure at 900°C⁵.

Battelle, LLC for financially sponsoring this work. The authors also acknowledge the contributions of Mattison Ferber, Robert Moore, and Jeffrey D. Smith to this work and the review of this manuscript by Edgar Lara-Curzio and Todd Sanders.

REFERENCES

- ¹G. D. DuVierre, A. Zanoli, Y. Boussant-Roux, and M. Nelson, "Selection of Optimum Refractories for the Superstructure of Oxy-Fuel Glass Melting Furnaces", *Ceramic Engineering Science Proceedings: 57th Conference on Glass Problems*. Vol. 18, No. 1, (1997).
- ²Crown Refractories for Glass Manufacturing with Oxygen-Fuel Combustion. Teltech Resource Network Corporation, (1996).
- ³H. T. Godard, L. H. Kotaeska, J. F. Wosinski, S. M. Winder, A. Gupta, K. R. Selkregg, and S. Gould, "Refractory Corrosion Behavior Under Air-Fuel and Oxy-Fuel Environments", *Ceramic Engineering Science Proceedings: 57th Conference on Glass Problems*. Vol. 18, No. 1, (1997).
- ⁴D. A. Porter and K. E. Easterling, *Phase Transformations in Metals and Alloys*. Second Edition, Chapman and Hall, (1992).
- ⁵J. G. Hemrick, "Creep Behavior and Physical Characterization of Fusion-Cast Alumina Refractories", Ph.D. Dissertation, University of Missouri-Rolla (2001).
- ⁶R. W. Brown, "Chapter 23 Applications of Fused Cast Alumina Refractories in the Glass Industry", *Refractories in the Glass Industry*; compiled by: A. G. Pincus, Magazines for Industry, Inc., (1980).
- ⁷J. G. Hemrick and A. A. Wereszczak, "Creep Measurement and Analysis of Refractories", *Fundamentals of Refractory Technology*. *Ceram. Trans.*, Vol. 125, (2001).
- ⁸A. A. Wereszczak, M. Karakus, K.C. Liu, B. A. Pint, R. E. Moore, and T. P. Kirkland, "Compressive Creep Performance and High Temperature Dimensional Stability of Conventional Silica Refractories", ORNL/TM-13757, (1999).
- ⁹W. D. Kingery, H. K. Bowen, and D. R. Uhlmann, *Introduction to Ceramics*. 2nd Edition, John Wiley & Sons, Inc. (1976).
- ¹⁰O. D. Slagle, "Thermal Expansion Hysteresis in Polycrystalline Graphite", *Carbon*, Vol. 7, pp. 337-344, (1969).
- ¹¹J. A. Kuszyk and R. C. Bradt, "Influence of Grain Size on Effects of Thermal Expansion Anisotropy in $MgTi_2O_5$ ", *J. Am. Ceram. Soc.*, **56**, [8] 420-423 (1973).
- ¹²E. D. Case, J. R. Smyth, and O. Hunter, "Grain-size Dependence of Microcrack Initiation in Brittle Materials", *J. Mater. Sci.*, **15**, pp. 149-153, (1980).
- ¹³E. D. Case, J. R. Smyth, and O. Hunter, "Microcracking in Large-grain Al_2O_3 ", *Mater. Sci. Eng.*, Vol. 51, pp. 175-179, (1981).
- ¹⁴T. E. Adams, D.J. Landini, C. A. Schumacher, and R. C. Bradt, "Micro- and Macrocrack Growth in Alumina Refractories", *Am. Ceram. Soc. Bull.*, **60** [7] (1981).
- ¹⁵"Standard Test Method of Measuring the Thermal Expansion and Creep of Refractories Under Load," ASTM C832, Vol. 15.01, American Society for Testing and Materials, West Conshohocken, PA, (1998).
- ¹⁶K. C. Liu, C. O. Stevens, C.R. Brinkman, and N. E. Holshauser, "A Technique to Achieve Uniform Stress Distribution in Compressive Creep Testing of Advanced Ceramics at High Temperatures," *Journal of Engineering for Gas Turbines and Power*, Vol. 119, (1997).
- ¹⁷K. C. Liu and J. L. Ding, "Mechanical Extensometer for High-Temperature Tensile Testing of Ceramics," *Journal of Testing and Evaluation*, No. 2, (1993).
- ¹⁸A. F. Wells, *Structural Inorganic Chemistry*, Fifth Edition, Oxford University Press (1975).
- ¹⁹R. W. Brown, "Chapter 24 Fused Cast Refractories", *Refractories in the Glass Industry*, compiled by: A.G. Pincus, Magazines for Industry, Inc., (1980).
- ²⁰S. I. Warshaw and F. H. Norton, "Deformation Behavior of Polycrystalline Aluminum Oxide", *J. Am. Ceram. Soc.*, **45** [10] 479-486 (1962).
- ²¹D. P. H. Hasselman and J. P. Singh, "Analysis of Thermal Stress Resistance of Microcracked Brittle Ceramics", *Am. Ceram. Soc. Bull.*, **58** [9] 856-860 (1979).
- ²²R. C. Stiffler and D. P. H. Hasselman, "Shear Moduli of Composites with Elliptical Inclusions", *J. Am. Ceram. Soc.*, **66** [3] C52-53 (1983).
- ²³E. A. Bush and F. A. Hummel, "High-Temperature Mechanical Properties of Ceramic Materials: I", *J. Am. Ceram. Soc.*, **41** [6] 189-95 (1958).
- ²⁴B. Budiansky and R. J. O'Connell, "Elastic Moduli of a Cracked Solid", *Int. J. Solids Struct.*, **12** [1] 81-97 (1976).
- ²⁵M. Dewey, "Elastic Constants of Materials Loaded with Non-Rigid Fillers", *J. Appl. Phys.*, **18** [6] 578-581 (1947).
- ²⁶Z. Hashin, "Elastic Moduli of Heterogeneous Materials", *J. Appl. Mech.*, **29** [1] 143-150 (1962).
- ²⁷A. Venkateswaran, K. Y. Donaldson, and D. P. H. Hasselman, "Role of Intergranular Damage-Induced Decrease in Young's Modulus in the Nonlinear Deformation and Fracture of an Alumina at Elevated Temperatures", *J. Am. Ceram. Soc.*, **71** [7] (1988).